Photorefractive Polymers. 2. Structure Design and Property Characterization

Luping Yu,* Waikin Chan, and Zhenan Bao

Department of Chemistry, The University of Chicago, 5735 South Ellis Avenue, Chicago, Illinois 60637

Simon X. F. Cao†

Department of Electrical Engineering, University of Florida, Gainesville, Florida 32611

Received October 8, 1992; Revised Manuscript Received January 26, 1993

ABSTRACT: To manifest a photorefractive effect, the polymer must possess a photocharge generator, a charge transporter, a charge trapping center, and a nonlinear optical (NLO) chromophore. We have synthesized novel photorefractive polymers which contain the NLO chromophore, the charge generator, and the transporting compound covalently linked to the polymer backbone. The charge generators absorbed strongly in the visible region (550–600 nm), allowing us to excite the species with normal laser sources. The other species had absorptions below 450 nm avoiding spectral overlap of these species with the charge generator. Structural characterizations confirmed that all of the species were incorporated into the polymer chains. These polymers exhibit relatively large electrooptical effects (r_{33} = 12.2 and 13.0 pm/V for polymers 1 and 2, respectively). A photocurrent of 1.4 μA was observed with a response time of 100 ms. Two beam coupling experiments revealed that the refractive index grating caused by the space charge field with a phase shift of 90° is a major contribution to the optical gain, which is a demonstration of the photorefractive effect.

Introduction

Since the advent of lasers, nonlinear optics has become one of the most extensively studied and influential fields in modern science and technology.[1] Various nonlinear optical (NLO) phenomena have been discovered and investigated in detail. Among them, the photorefractive (PR) effects have attracted considerable attention due to their potential applications in, e.g., image amplification, phase conjugation, three-dimensional optical data storage, real-time image processing, and programmable interconnection.[2–5] The photorefractive (PR) effect involves a change in the index of refraction. The unique feature of the photorefractive effect is that it is a nonlocal effect, creating very large index changes via the linear electrooptical effect (Pockel effect) which is modulated by a photoinduced space charge field.[3,4] One of the effects of the dynamic changes of the index of refraction is that a very efficient energy transfer between the light beams can occur, resulting in two-beam coupling.

In order to manifest the photorefractive effect, the materials must be noncentrosymmetric and photoconductive. Therefore, extensive studies have been focused on inorganic single crystals with noncentrosymmetric structures, such as ferroelectric crystals ($LiNbO_3$, $LiTaO_3$, $BaTiO_3$) and semiconductors (GaAs, InP, CdF_2).[2–5] However, the commercialization of photorefractive technology based on these materials has been hindered by the difficulty of preparing and processing them.

Photorefractive effects have been observed in both doped organic crystals and polymers.[6,7] Compared to inorganic photorefractive materials, organic photorefractive materials have very attractive features, including their reasonably large electrooptic response, their low dielectric constant, their versatility in choosing photocarrier generators and trappers for different frequency requirements, and their good processibility for device fabrications. However, materials reported so far are organic single crystals doped with a charge generator and polymer composite systems which are obviously not optimized.[6,7] The growing of a doped organic single crystal is a very difficult process because of the incompatibility of dopants with the crystal structure. In composite materials, there are problems such as phase separation and the instability of the NLO activity due to relaxation. Therefore, new materials with enhanced PR effects and improved properties are required. Recently, we have succeeded in preparing a new photorefractive polymer with an NLO chromophore, a photocarrier generator, and a transporting compound covalently linked to its backbone,[8] in contrast to the doped systems reported in the literature.[6] This paper reports an extended study of the synthesis and physical characterization of new photorefractive polymers, whose structures are represented in Scheme I.

Experimental Section

3,3′-Dimethoxy-4,4′-diisocyanatobisphenyl (Pfaltz and Bauer Chemical Co.) was purified by recrystallization from dried hexane. Dimethylformamide (DMF) was purified by distillation over phosphorus pentoxide. All of the other chemicals were purchased from the Aldrich Chemical Co. and were used as received unless otherwise stated. The structures of various monomers are shown in Scheme I, and their synthetic approaches are shown in Scheme II.

Synthesis of Monomers. Compound 4. Benzyl chloride (38.4 mL, 0.34 mol) was added dropwise to a solution of aniline-*N*,*N*-diethanol (30 g, 0.17 mol) and triethylamine (60 mL) in THF (150 mL). The resulting mixture was stirred at room temperature for 2 h and then poured into water (500 mL). The yellow oily liquid precipitated and solidified on standing. The solid was filtered off and recrystallized from methanol to yield white crystals (58.6 g, 91%, mp 72.0–73.5 °C). ^{1}H NMR ($CDCl_3$): δ 3.82 (t, J = 6.6 Hz, 4 H, $-NCH_2-$), 4.52 (t, J = 6.6 Hz, 4 H, $-CH_2O-$), 6.71–7.97 (m, 15 H, aromatic protons).

Compound 5. Phosphorus oxychloride (4.79 mL, 51.4 mmol) was added dropwise to DMF (10 mL) at 0 °C, and the resultant solution was stirred for 1 h at 0 °C and for another 1 h at 25 °C. Compound 4 (20 g, 51.4 mmol) in DMF (10 mL) was then added slowly to the solution, and the mixture was further heated at 90 °C for 6 h. After completion of the reaction, the mixture was poured into crushed ice (50 g) and extracted with methylene chloride three times (a potion of 50 mL). The organic layer was washed with a saturated sodium bicarbonate solution and water

† Present address: E-TEK Dynamic Inc., 1885 Lundy Ave., San Jose, CA 95131.

0024-9297/93/2226-2216$04.00/0

Scheme I
Syntheses of Photorefractive Polymers

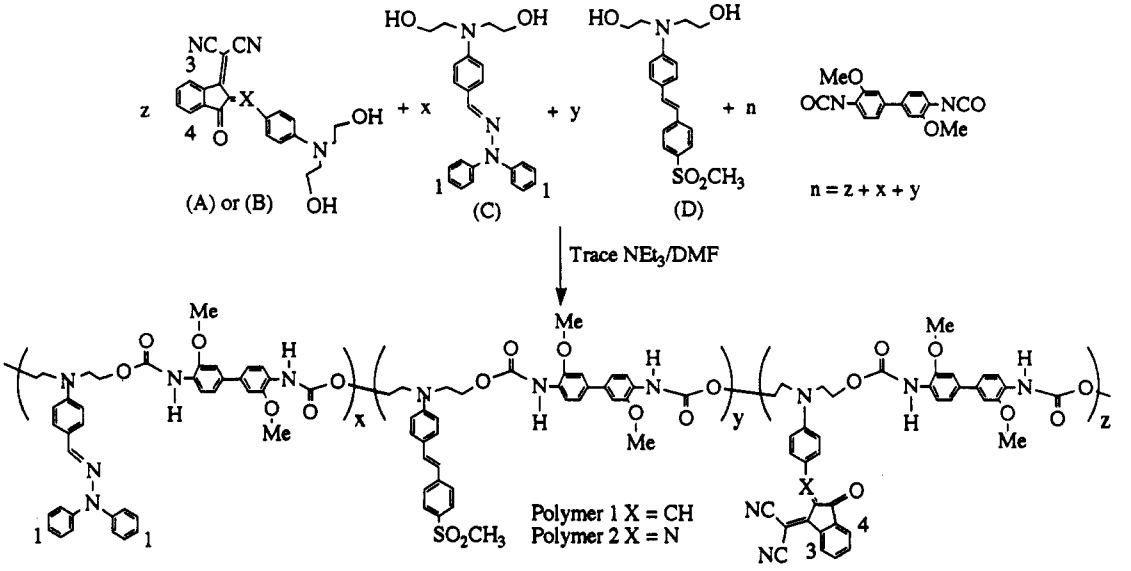

Scheme II
Syntheses of Monomers

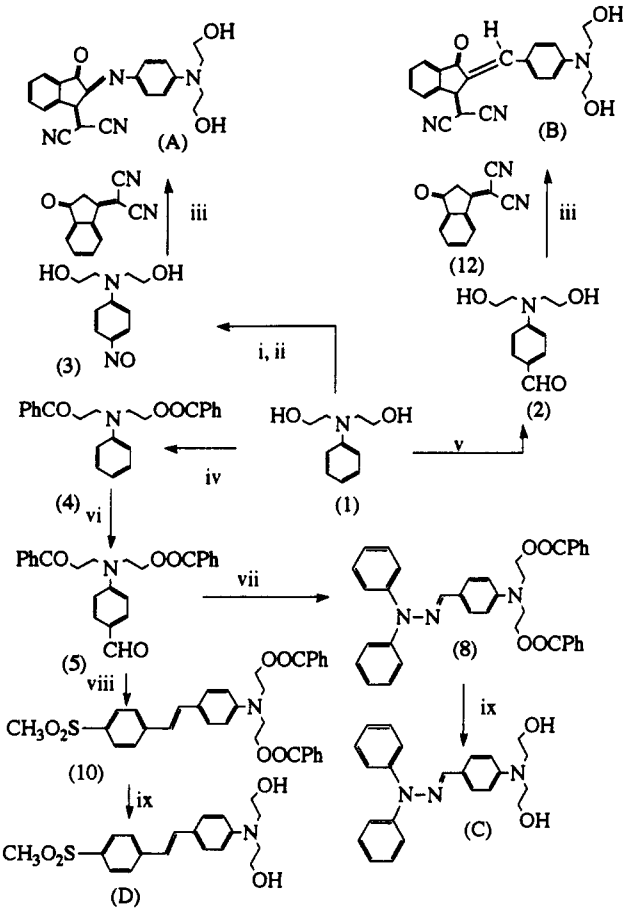

Reaction Conditions

i. $NaNO_2$, HCl ii. Na_2CO_3 iii. $EtOH/CH_2Cl_2$ iv. $PhCOCl$, NEt_3 v. $(CH_2NH)_6$, HCOOH, EtOH vi. DMF, $POCl_3$ vii. Ph_2NNH_2, NaOAC viii. (CH_3O_2S)-Ph-$CH_2P(O)(OEt)_2$, NaH, glyme; ix. $NaOH/H_2O$/EtOH

(twice) and dried over magnesium sulfate. The solvent was removed under reduced pressure. The crude product was recrystallized from methanol, obtaining a white solid (16.7 g, 78%, mp 78.0–79.5 °C). ^1H NMR ($CDCl_3$): δ 3.93 (t, J = 5.9, 4 H, $-NCH_2-$), 4.56 (t, J = 5.9, 4 H, $-CH_2O-$), 6.94–7.99 (m, 14 H, aromatic protons), 9.76 (s, 1 H, –CHO).

Monomer A. A mixture of compound **3**[9] (3.500 g, 16.67 mmol) and 3-(dicyanovinyl)indan-1-one (compound **12**[13] 3.000 g, 15.96 mmol) in ethanol/methylene chloride (20 mL/10 mL) was stirred at room temperature for 5 h. The suspension was filtered, and the solid was washed with ethanol until the filtrate turned blue. The product was recrystallized from ethanol (4.78 g, 84% based on compound **12**, mp 216–218 °C). ^1H NMR (DMSO-d_6): δ 3.6–3.7 (m, 8 H, $-CH_2CH_2-$), 4.8 (t, J = 4 Hz, 2 H, OH), 6.95–8.5 (m, 8 H, aromatic protons). MS: m/z 386, 368, 355, 296. Anal. Calcd for $C_{22}H_{18}N_4O_3$: C, 68.39; H, 4.66; N, 14.51. Found: C, 68.57; H, 5.01; N, 14.43.

Monomer B. This compound was synthesized from compounds **2** and **12** in a procedure similar to that for monomer A. ^1H NMR (DMSO-d_6): δ 3.6–3.8 (m, 8 H, $-CH_2CH_2-$), 6.95–8.5 (m, 9 H, aromatic and vinyl protons). Anal. Calcd for $C_{23}H_{19}N_3O_3$: C, 71.69; H, 4.94; N, 14.61. Found: C, 71.54; H, 4.87; N, 14.72.

Monomer C. The mixture of compound **5** (6.00 g, 20 mmol), 1,1-diphenylhydrazine hydrochloride (0.44 g, 20 mmol), sodium acetate (1.8 g, 22 mmol), and ethanol (50 mL) was stirred at room temperature for 2 h. A sodium hydroxide solution (20%, 20 mL) was added, and the reaction mixture was further stirred at room temperature overnight. The product crystallized out during stirring and was filtered off. After washing it with water three times, the solid was recrystallized from methanol (6.5 g, 72%, mp 124.5–125.5 °C). ^1H NMR (DMSO-d_6): δ 3.4 (t, J = 6 Hz, 4 H, $-NCH_2-$), 3.6 (t, J = 6 Hz, 4 H, OCH_2-), 4.75 (t, J = 4 Hz, 2 H, OH), 6.6–7.4 (m, 15 H, aromatic proton and –CH=N–). MS: m/z 375, 357, 344, 169. Anal. Calcd for $C_{23}H_{25}N_3O_2$: C, 73.60; H, 6.67; N, 11.20. Found: C, 73.35; H, 6.76; N, 11.06.

Monomer D. This compound was prepared according to the literature procedure with modifications.[10] In a 250-mL round-bottomed flask flushed with nitrogen, the mixture of compound **5** (14.53 g, 34.8 mmol), sodium hydride (2.50 g, 104.0 mmol), and 1,2-dimethoxyethane (glyme, 80 mL) was stirred for 5 min. To this solution was added diethyl-4-(methylsulfonyl)benzyl phosphonate (10.65 g, 34.8 mmol) in glyme (40 mL). The resultant mixture was heated under reflux for 2 h and then poured over crushed ice (200 g) under nitrogen. The viscous material was isolated and dissolved in ethanol (60 mL). To this solution was added a sodium hydroxide solution (4 g in 15 mL of water), and the mixture was heated to reflux overnight. After cooling, the yellow solid was filtered off and washed with water three times. The crude product was further recrystallized from methanol (3.49, 28%, mp 278–280 °C). ^1H NMR (DMSO-d_6): δ 3.1 (s, 3 H, $-SO_2-CH_3$), 3.4 (t, J = 6 Hz, 4 H, $-NCH_2-$), 3.6 (t, J = 6 Hz, 4 H, OCH_2-), 4.75 (t, J = 4 Hz, 2 H, OH), 6.7, 7.4, 7.7, 7.8 (m, 8 H, aromatic proton), 7.0 and 7.3 (d, 10 Hz, 2 H, vinyl proton). MS: m/z 361, 343, 330, 300, 286, 207, 178. Anal. Calcd for $C_{19}H_{23}-NO_4S$: C, 63.16; H, 6.37; N, 3.88. Found: C, 62.96; H, 6.71; N, 3.59.

Polymerization. In a typical polymerization, a mixture of monomers A (0.3208 g, 0.831 mmol), C (0.3116 g, 0.831 mmol),

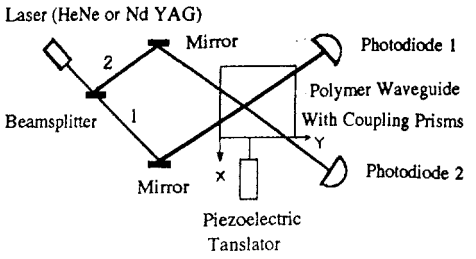

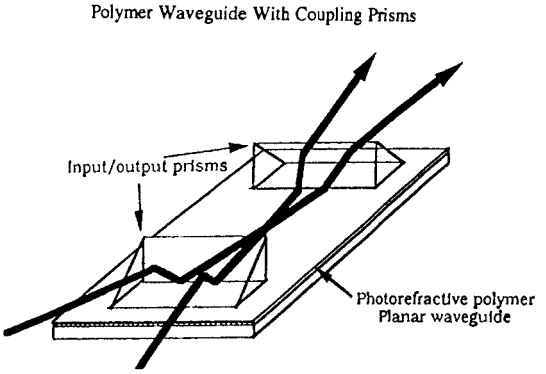

Figure 1. Experimental setup of two-beam coupling experiments and the structure of the polymer waveguide with coupling prisms.

and D (0.3000 g, 0.831 mmol) and 3,3′-dimethoxy-4,4′-diisocyanatobiphenyl (0.7380 g, 2.493 mmol, as comonomer) was dissolved in DMF (20 mL), and 2 drops of triethylamine was added to facilitate the polymerization. The resultant mixture was heated to 90 °C for 2 h and was then poured into methanol. The polymer was filtered off and washed with methanol until colorless. It was further purified by extraction in a Soxhlet extractor with methanol under the wrap of aluminum foils. Then it was dried under vacuum at 50 °C for 2 days. ^{1}H NMR spectra are shown in Figure 6.

The FTIR spectra were taken with a Nicolet 20 SXB FTIR spectrometer, and the UV/vis spectra were taken by using a Perkin-Elmer Lambda 6 UV/vis spectrophotometer. Thermal analyses were performed using DSC-10 and TGA-50 systems of TA Instrument with a heating rate of 10 °C/min. NMR spectra were recorded on a GE, Omega 500-MHz NMR spectrometer. Molecular weights were measured with a Waters RI GPC system using polystyrene as the standards.

Physical Measurements. After spin coating the polymer onto the indium–tin oxide (ITO) glass slide, gold electrodes were deposited on the polymer surface. Photoconductivity measurements were performed by monitoring the photocurrent response of the polymer sample (90 μm) to a laser beam at 632 nm with an intensity of 0.4 W/cm^2. The electrooptic effect in the polymer was studied by using an interferometry method at 632 nm.[11] The dielectric constant was determined by measuring the capacitance of the ITO–polymer–gold structure as described in the literature.[12]

In order to characterize the mechanism of the photoinduced grating in the polymers, two-beam coupling experiments were performed. Due to the difficulties of fabricating a polymer film of uniform thickness, a planar waveguide geometry was chosen to increase the grating interaction length. The experimental setup is shown in Figure 1 where a HeNe laser has been used as the light source. The output of the HeNe laser was split into two beams of equal intensity. These two parallel collimated beams were simultaneously coupled into the polymer planar waveguide by a prism and intersected with each other with an angle of 2θ inside the waveguide. Finally, the two separated beams were coupled out of the polymer waveguide by another prism and sent to two calibrated photodiodes. The combined prisms and waveguide coupling apparatus was mounted on a piezoelectrically driven translation stage and a step motor-driven rotation stage. The polymer waveguides consisted of a 0.8-μm-thick spin-coated polymer film on an ITO glass substrate with a 100-nm-thick SiO_2 buffer layer. The experiments were performed on both poled and unpoled samples.

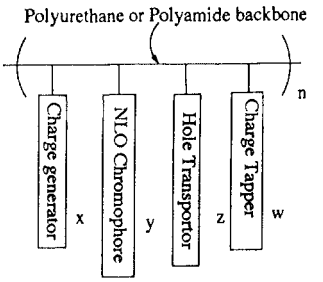

Figure 2. Schematic structure of the target photorefractive polymers.

Results and Discussion

Structural Characterization. Our target photorefractive polymer had a structure as shown in Figure 2, where four different species are incorporated into the polymer backbone. However, in the first such polymer, we intentionally did not incorporate the charge trapping center. The trapping centers naturally exist in the polymer sample due to defects and conformational disorders as pointed out by Ducharme et al.[6] Our experiments, to be discussed later, demonstrated the existence of the trapping center. Our reaction scheme offers the flexibility of deliberately incorporating different trapping centers onto the polymer backbone. A detailed study of this aspect is still in progress and will be reported later.

When selecting different species, an important consideration was the absorption windows of different species. We chose the charge generator absorbing at long wavelengths (say, above 500 nm) so that a normal laser light can be used to excite the species. Also, we chose the charge transporting compound and the NLO chromophore to absorb below 450 nm, so that when the charge generator is excited, the other species are in the dark region. This is shown in the absorption spectra of our monomers (see Figure 3). Figure 3 shows that the UV/vis spectrum of the charge generator has a strong absorption at 550 nm for monomer B and at 600 nm for monomer A. The absorptions of the NLO chromophore and the transporting compound appear at 380 nm.

The polymerization was carried out in the purified DMF under a nitrogen atmosphere (see Scheme I). Polymer 1 is a red-purple powder, and polymer 2 is a blue powder. They are soluble in a variety of organic solvents, such as chloroform, THF, DMF, etc. The GPC measurements in THF, using polystyrene as the standard samples, indicated a weight-average molecular weight of about 5000–20 000 with a polydispersity of ca. 2.1–2.5. Optical quality films can be cast from the polymer solution.

Both polymers have similar thermal properties; TGA studies showed that they are stable up to 250 °C under a nitrogen atmosphere (Figure 4). Since the polymer has a polyurethane structure, hydrogen bonds exist among the imide groups. This is reflected in the high T_g values of the polymers, around 146 °C (see Figure 5). These thermal properties indicate that the polymer can be electrically poled at ca. 145 °C without damaging the materials.

The structural information of these polymers was provided by ^{1}H NMR, FTIR, and UV/vis spectroscopic results. The NMR spectra clearly indicate that all of the three species were indeed incorporated into the polymer chain (see Figure 6). For example, in the NMR spectrum of polymer 1, the following characteristic chemical shifts were observed: δ 3.02 (SO_2CH_3), 3.7 ($-NCH_2-$), 3.85 ($-OCH_3$), 4.4 ($-OCH_2-$), 8.6 (proton 3), 6.75 (proton 1, see Scheme II for the numbering). The integrations of the corresponding protons indicated the composition of the polymer ($[NLO]_{0.9/2.9}[G]_{1/2.9}[T]_{1/2.9}[COM]_n$), where NLO,

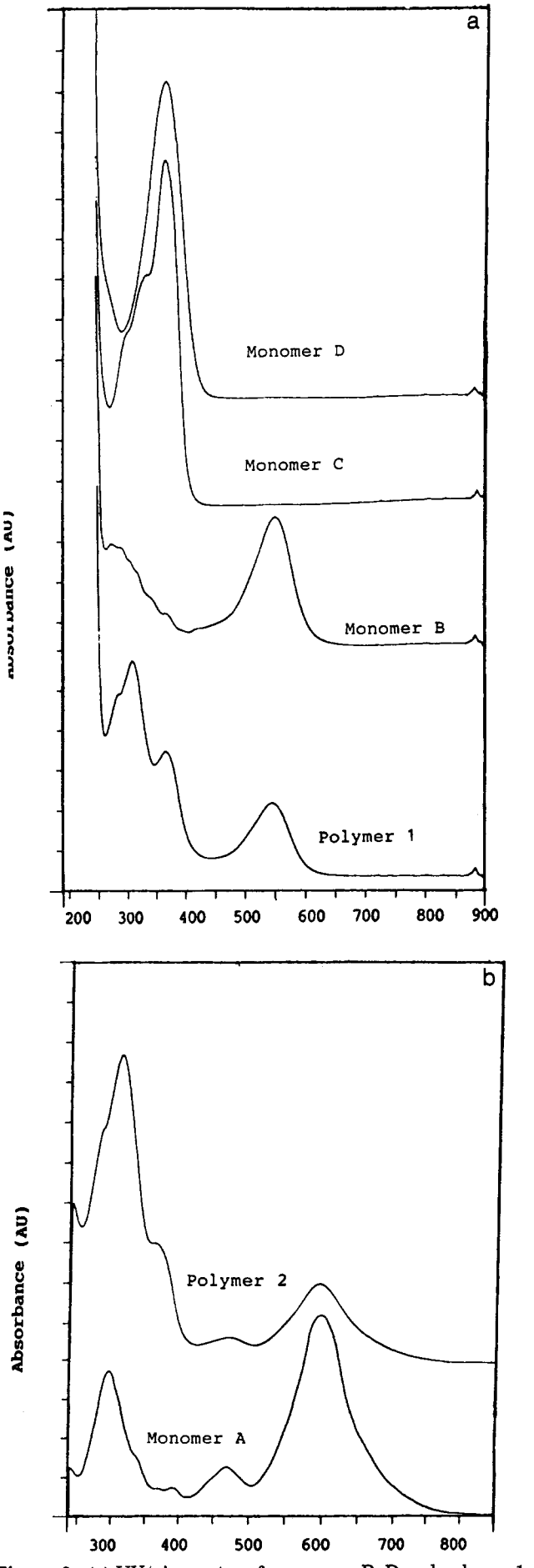

Figure 3. (a) UV/vis spectra of monomers B–D and polymer 1 in chloroform. (b) UV/vis spectra of monomer A and polymer 2 in chloroform.

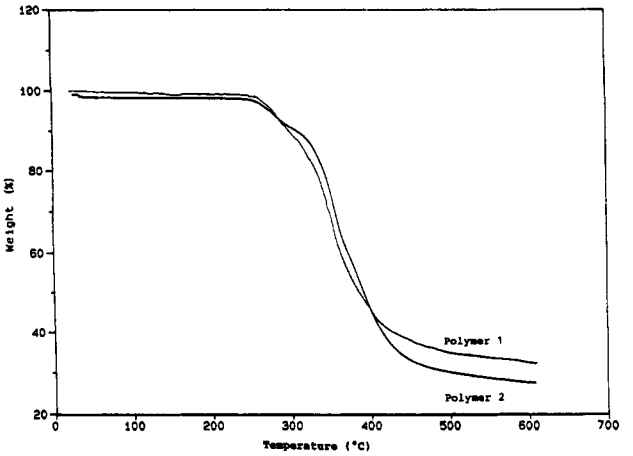

Figure 4. TGA diagrams of polymers 1 and 2, at a heating rate of 10 °C/min.

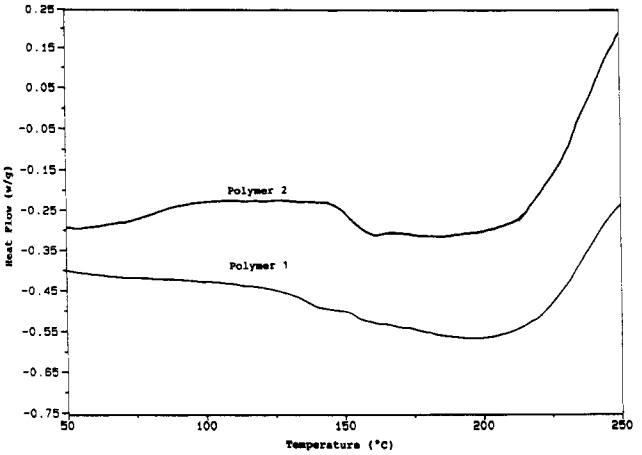

Figure 5. DSC traces of the polymers 1 and 2, at a heating rate of 10 °C/min.

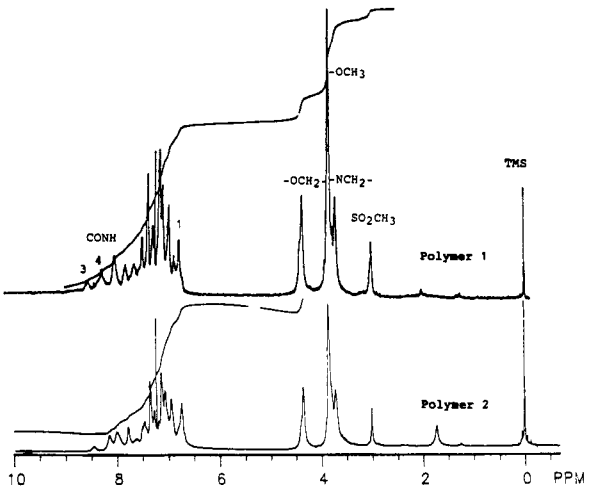

Figure 6. ^1H NMR spectra of polymers 1 and 2 in $CDCl_3$.

G, T, and COM stand for the NLO chromophore, the charge generator, the charge transporting compound, and the comonomer, respectively. This result is consistent with the ratios of the starting monomers ($[NLO]_1[G]_1[T]_1[COM]_3$). Similar results were deduced for polymer 2.

The FTIR spectra of these two polymers showed absorptions of the N–H band at 3520 cm^{-1}, the CH_2 band around 2850 cm^{-1}, the –CN band around 2236 cm^{-1}, and the C=O band at ca. 1727 cm^{-1}. Special bands for the monosubstituted phenyl ring in the transporting compound (monomer C) appeared at 715, 738, and 834 cm^{-1}.[14]

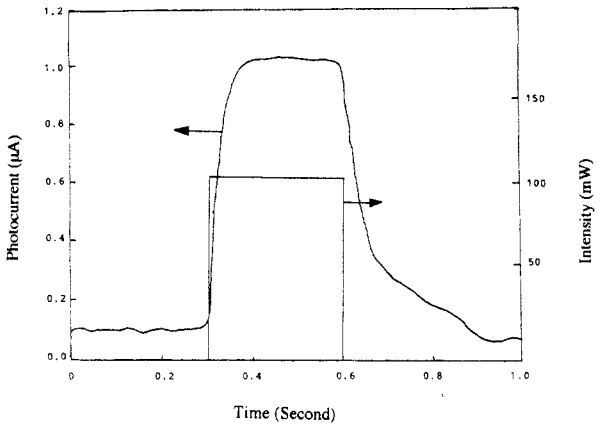

Figure 7. Photocurrent response profile of polymer 1. A HeNe laser was used to excite the polymer samples.

The UV/vis spectra (see Figure 3) of the polymers showed the typical absorption of the charge generators at 550 nm for polymer 1 and at 600 nm for polymer 2. It should be noted that the maximum absorption wavelength of the charge generators did not change significantly, which indicated that there were no charge-transfer complexes formed between the charge generator and the various other species. The absorptions of the NLO chromophore and the transporting compound appeared at 380 nm which is similar to those of the corresponding monomers.

Physical Characterization. To achieve the charge separation, the materials must be photoconductive. Photoconductivity measurements of the polymers were performed by monitoring the photocurrent response to a laser beam at 632 nm. A typical photoresponse profile for polymer 1 is shown in Figure 7 from which a response time of 100 ms can be deduced. A maximum photocurrent of 1.5 μA was observed with an applied electric field of 100 V and a laser intensity of 0.4 W/cm^2, while the dark current is very small and barely detectable. The quantum yield of the photocharge generation was calculated to be ca. 2.6 $\times$ 10^{-3} charges photon.

The pristine polymer thin film has a random dipole orientation. To introduce the asymmetry, the polymer films were electrically poled at 145 °C in a waveguide structure (poling field, 70 V/μm). The electrooptic effect in the polymer was studied following the literature method using a HeNe laser beam;[12] electrooptic coefficients, r_{33}, of 12.2 and 13.0 pm/V were detected for polymers 1 and 2, respectively. One of the advantages of these polymers is that, due to the hydrogen bonding, the E–O coefficients in these polymers were quite stable; a value of 11.6 pm/V was detected 3 months after poling for polymer 1 (see Figure 8).

In order to confirm the photorefractive effect, a distinctive experiment is the two-beam coupling experiment. This involves the "writing" of a hologram by the two beams intersecting in the polymer and the coupling of the same beams by the hologram formed, resulting in an optical energy exchange between the two beams. By monitoring this optical energy exchange, one can deduce the optical gain coefficient which is proportional to the internal field (E_{sc}) induced by the separated charges. To perform the two-beam coupling experiment, the sample must be sufficiently thick for the formation of an efficient grating. Since the thickest polymer film prepared was ca. 90 μm which is still not thick enough to detect efficient energy transfer, we carried out this experiment in a waveguide structure using a HeNe laser. In the waveguide structure, we used a film with a thickness of 0.8 μm. The experimental setup is shown in Figure 1 where the two beams

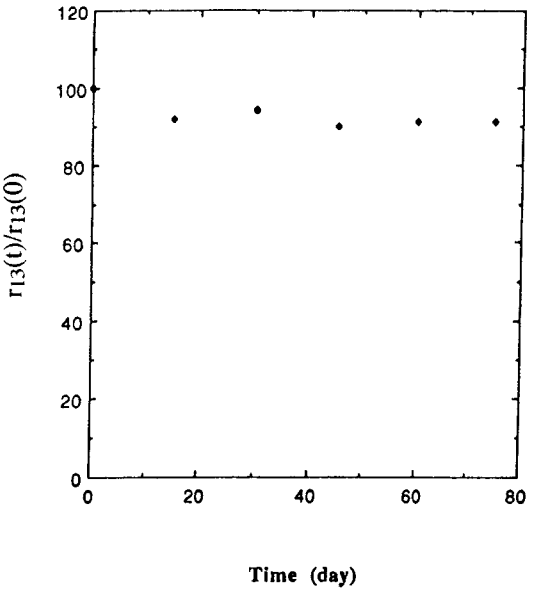

Figure 8. Temporal stability of the electrooptical coefficient r_{13} of polymer 1.

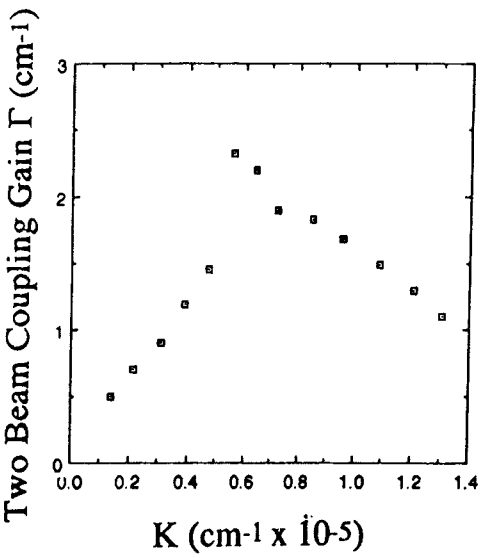

Figure 9. Two-beam coupling gain Γ as a function of the grating vector K.

have enough interaction distance (3 mm) to form an interference pattern. The propagation direction of the laser beams was designated as the y direction, and the **K** vector is in the x direction. Figure 9 shows the two-beam coupling gain of polymer 1 as a function of the grating wave number K (=$(4\pi/\lambda)\sin(\theta/2)$), where θ is the beam intersecting angle outside of the waveguide.

It is known from band transport theory that the steady-state two-beam coupling gain can be related to the grating wavenumber by[2,15]

$$K/\Gamma = (\lambda e/2\pi n^3 K_B T r_{eff})(1 + K^2/K_s^2) \quad (1)$$

where K_s is the Debye screening wave vector and equals $(e^2 N_E/\epsilon\epsilon_0 K_B T)^{1/2}$, N_E is the effective number of empty traps [$N_E = (NN^+)/(N+N^+)$], K_B is Boltzmann's constant, ϵ is the relative dielectric constant, and r_{eff} is the effective electrooptic coefficient ($r_{eff} = F\sigma r_A$, where r_A is the electrooptic coefficient measured by experiment, σ is the relative contribution of the hole and electron carrier to the photorefractivity, and F is the fractional poling factor). If r_{eff} is independent of K, a plot of K/Γ vs K^2 should be linear, with an intercept from which r_{eff} can be deduced and a slope/intercept ratio from which K_s can be deduced.

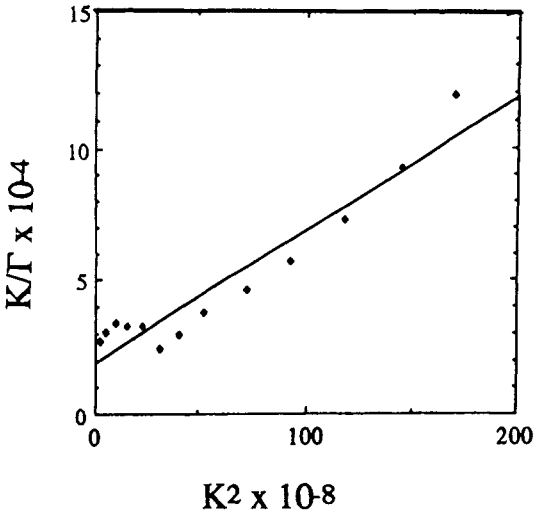

Figure 10. Experimental data fit based on the band transporting theory, K/Γ vs K^2.

Figure 10 shows such a plot, where the data points deviate from a linear relationship. If we fit the data to a straight line, we obtain an N_E value of 2.6×10^{15} (cm^{-3}) and a r_{eff} value of 2.8 pm/V. However, after examining the data more carefully, we found that more than one process is involved in the photorefractive effect.

In order to determine the contributions of different mechanisms, we performed the two-beam coupling experiments by attaching a piezoelectric transducer to the polymer waveguide sample so as to create a small displacement between the intensity grating and the index grating.[7,16] The experiments were performed on polymer waveguide samples with and without corona poling.

In the unpoled polymer waveguide sample, only the absorption grating was observed. This absorption grating has a long buildup time, and the light diffraction from it is independent of the writing beam polarization. We also observed that the diffraction efficiency decreased after multiple writings, indicating that most of the photoinduced absorption change is permanent. On the basis of these observations, the origin of this absorption grating can be attributed to a photochromic effect.

In the vertically poled (normal to the waveguide plane) sample, both phase and absorption gratings were observed. The absorption grating is about the same amplitude as the unpoled sample. The phase shift of the absorption grating, ϕ_a, was determined to be $0 \pm 20°$; that of the phase grating, ϕ_p, was about $26 \pm 20°$. Even though we did not observe a completely asymmetrical energy transfer between the two beams, the results observed strongly indicated that the observed beam coupling is due to the electrooptic effect caused by the photoinduced space charge field. The detailed experimental results and an explanation will be presented elsewhere.[17]

Conclusion

We have synthesized the first polymeric photorefractive materials which contain a photocarrier generator, a hole transporting compound, and a nonlinear optical chromophore, covalently linked to polymer backbones. The two-beam coupling experiments in a waveguide structure allowed us to distinguish the contribution of different mechanisms. The experimental results demonstrated that the major contribution of the photorefractive effect comes from the space field due to the light-induced charge separation with a subsequent electrooptic refractive index change.

Acknowledgment. L.Y. thanks the Camille & Henry Dreyfus Foundation for support through a New Faculty Award. Acknowledgement is also made to the donors of the Petroleum Research Fund, administered by the ACS, for partial support of this research.

References and Notes

(1) Shen, Y. R. *The Principles of Nonlinear Optics*; John Wiley & Sons: New York, 1984.
(2) Gunter, P., Huiguard, J. P., Eds. *Photorefractive Materials and Their Applications*; Springer-Verlag: Berlin, 1988; Vols. I and II.
(3) Yariv, A. *Optical Electronics*, 4th ed.; Saunders College Publishing: Philadelphia, PA, 1991.
(4) Weiss, S.; Fisher, B. *Opt. Quantum Electron.* **1990**, *22*, S17.
(5) Feinberg, J.; Heiman, D.; Tanguay, A. R., Jr.; Hellwarth, R. W. *Appl. Phys.* **1980**, *51*, 1299.
(6) Ducharme, S.; Scott, J. C.; Twieg, R. J.; Moerner, W. E. *Phys. Rev. Lett.* **1991**, *66*, 1846.
(7) Sutter, K.; Hullinger, J.; Gunter, P. *Solid State Commun.* **1990**, *74*, 867.
(8) Yu, L. P.; Chan, W. K.; Bao, Z. N.; Cao, S. X. F. *J. Chem. Soc., Chem. Commun.* **1992**, 1735.
(9) Sen, A. K.; Price, C. C. *J. Org. Chem.* **1959**, *24*, 125.
(10) Ulman, A.; Wiland, C. S.; Kohler, W.; Robello, D. R.; William, D. J.; Handley, L. *J. Am. Chem. Soc.* **1990**, *112*, 7083.
(11) Kobayashi, T. *Nonlinear Opt.* **1991**, *1*, 239.
(12) Schidkraunt, J. S. *Appl. Phys. Lett.* **1991**, *58*, 340.
(13) Bello, K. A.; Cheng, L.; Griffiths, J. *J. Chem. Soc., Perkin Trans. 2* **1987**, 815.
(14) Pretsch, E.; Seibl, J.; Simon, W.; Clerc, T. *Table of Spectra Data for Structure Determination of Organic Compounds*; Springer-Verlag: Berlin, 1983.
(15) Klein, M. B. Reference 2, Chapter 7.
(16) Kogelnik, H. *Bell Syst. Tech. J.* **1969**, *48*, 2909.
(17) Yu, L. P.; Cao, S. X. F. *Appl. Phys. Lett.* Manuscript in preparation.